

Inhibition of CO₂ fixation by iodoacetamide stimulates cyclic electron flow and non-photochemical quenching upon far-red illumination

Pierre Joliot · Jean Alric

Received: 25 November 2012 / Accepted: 8 April 2013 / Published online: 28 April 2013
© Springer Science+Business Media Dordrecht 2013

Abstract The Benson–Calvin cycle enzymes are activated *in vivo* when disulfide bonds are opened by reduction via the ferredoxin-thioredoxin system in chloroplasts. Iodoacetamide reacts irreversibly with free –SH groups of cysteine residues and inhibits the enzymes responsible for CO₂ fixation. Here, we investigate the effect of iodoacetamide on electron transport, when infiltrated into spinach leaves. Using fluorescence and absorption spectroscopy, we show that (i) iodoacetamide very efficiently blocks linear electron flow upon illumination of both photosystems (decrease in the photochemical yield of photosystem II) and (ii) iodoacetamide favors cyclic electron flow upon light excitation specific to PSI. These effects account for an NPQ formation even faster in iodoacetamide under far-red illumination than in the control under saturating light. Such an increase in NPQ is dependent upon the proton gradient across the thylakoid membrane (uncoupled by nigericin addition) and PGR5 (absent in *Arabidopsis pgr5* mutant).

Iodoacetamide very tightly insulates the electron current at the level of the thylakoid membrane from any electron leaks toward carbon metabolism, therefore, providing choice conditions for the study of cyclic electron flow around PSI.

Keywords Iodoacetate · NPQ · Pgr5 · Ferredoxin-thioredoxin activation · Benson–Calvin cycle

Introduction

Photosynthetic electron transfer in algae or plants can operate according to two modes: linear and cyclic electron flow. In the linear mode, electrons are transferred from water to NADP⁺ and then to the Benson–Calvin cycle via the three major complexes of the photosynthetic chain, photosystem (PS) II, cytochrome *b₆f* complex, and PSI. In the cyclic mode, which involves only PSI and cyt *b₆f* complexes, electron transfer is coupled to proton transfer and generates a transmembrane electrochemical proton gradient ($\Delta\mu\text{H}^+$) that leads to ATP synthesis (Arnon et al. 1954). It has been shown that illumination of dark adapted leaves leads to a rapid increase in their ATP concentration (Harbinson and Foyer 1991; Joliot and Joliot 2008). This cannot be solely due to linear electron transfer, because the Benson–Calvin cycle consumes slightly more ATP per NADPH than that produced by linear electron flow (Seelert et al. 2000; Allen 2003). Thus, the large increase in ATP concentration observed during the first minute of illumination is witness to the additional contribution of the cyclic process and possibly of the Mehler reaction. There is general agreement that cyclic electron flow obligatory involves cyt *b₆f* and PSI. In addition, the cyclic process involves electron transfer from NADPH or

Electronic supplementary material The online version of this article (doi:10.1007/s11120-013-9826-1) contains supplementary material, which is available to authorized users.

P. Joliot (✉) · J. Alric
Unité Mixte de Recherche 7141 CNRS-Université Paris 6,
Institut de Biologie Physico-Chimique, 13, rue Pierre et Marie
Curie, 75005 Paris, France
e-mail: pjoliot@ibpc.fr

J. Alric
e-mail: jean.alric@cea.fr

Present Address:

J. Alric
Service de biologie végétale et de microbiologie
environnementales—UMR 7265 (Cnrs/Cea/Aix-Marseille
Université) (SBVME), CEA Cadarache, Bât 177,
13108 St Paul Lez Durance, France

ferredoxin (Fd) to the plastoquinone pool. The low concentration of NADPH-dehydrogenase ($\sim 1\%$ of PSI (Sazanov et al. 1996)) may suggest that this pathway plays a minor role under strong illumination. A faster electron transfer may occur between reduced Fd, which binds to the stromal side of *cyt b₆f* complex, and plastoquinones (Joliot and Joliot 2002; Iwai et al. 2010).

After a longer period of illumination, a large variety of mechanisms protect the photosynthetic apparatus against a perceived excess of light. Such mechanisms, reviewed in (Horton et al. 1996), are referred to as non-photochemical quenching (NPQ) and are involved in the protection of the PSII centers and of the antenna localized in the appressed region of the membrane. Several NPQ components can be distinguished. (i) A major component, denoted qE, requires the presence of the PSBS subunit (Li et al. 2004) and is associated with the acidification of the lumen (Gilmore and Björkman 1995). Lumenal acidification induces the de-epoxidation of violaxanthin into zeaxanthin (xanthophyll cycle) (Siefermann and Yamamoto 1975) and a conformational change in the environment of zeaxanthin detected as a red shift in absorbance (Heber 1969; Ruban et al. 2002). This red shift is possibly associated with an electrochromic change induced by the protonation of protein residues localized in the vicinity of zeaxanthin. (ii) Another component, qT, reflects small changes in the relative size of PSII and PSI antenna (state transition (Allen 1992)). (iii) The last component, qI, is a slowly reversible process (>1 h), generally attributed to photoinhibition of PSII. The amplitudes of qT and qI are small compare to qE, and their relaxation in the dark is several orders of magnitude slower than qE.

Strong light also induces the oxidation of a large fraction of the primary electron donor of PSI, P₇₀₀ (Harbinson and Woodward 1987; Harbinson and Foyer 1991; Ott et al. 1999) that reflects a limitation of intersystem electron transfer at the level of *cyt b₆f*. Oxidation of P₇₀₀ to P₇₀₀⁺ protects PSI from photodamage by preventing the occurrence of back reactions that generate reactive oxygen species (Rutherford et al. 2012). The molecular basis of this limitation of intersystem electron transfer is that the proton gradient formed in the light slows down the rate of PQH₂ oxidation at the Q_o site of *cyt b₆f* (Kok et al. 1969; Finazzi and Rappaport 1998), accounting for the accumulation of P₇₀₀⁺ in the light (Harbinson and Woodward 1987; Harbinson and Foyer 1991; Ott et al. 1999). Addition of nigericin at low concentration (~ 1 μ M) dissipates the proton gradient Δ pH without drastically affecting the membrane electrochemical potential ($\Delta\mu$ H⁺) (Joliot and Johnson 2011). Expectedly, nigericin addition collapses most of the NPQ (Gilmore and Björkman 1995) but it also prevents the accumulation of P₇₀₀⁺ in the light (Joliot and Johnson 2011). As a consequence of nigericin addition, PSI

is prone to charge recombination and is rapidly photoactivated in the light (Joliot and Johnson 2011). Thus, under strong illumination, cyclic electron flow generates a proton gradient that protects both photosystems: PSII because NPQ decreases PSII antenna size, and PSI because *cyt b₆f* limits electron transfer at the donor side of PSI rather than at its acceptor side. It thus appears that the regulatory processes that control the bifurcation of electrons in the stroma between the cyclic and linear pathways play a key role in the adaptation of plants to changes in the light environment.

Hald et al. (2008) have compared wild-type tobacco leaves to mutants partially depleted in ferredoxin NADP⁺ reductase (FNR), involved in the oxidation of ferredoxin, and in glyceraldehyde phosphate dehydrogenase (GAPDH), which oxidizes NADPH. Under steady state illumination, the FNR mutant showed a lower amount of oxidized P₇₀₀ than the WT whereas the GAPDH mutant shows a larger P₇₀₀ oxidation. To account for the latter observations on P₇₀₀⁺, Hald et al. (2008) proposed that the reduction of the pool of NADP⁺ induced the down regulation of the *cyt b₆f* turnover in the WT. More recently it was shown in the FNR mutant that NPQ was largely inhibited as well as P₇₀₀ oxidation, suggesting that this enzyme is directly involved in the cyclic process (Joliot and Johnson 2011).

FNR and *cyt b₆f* were copurified (Clark et al. 1984; Zhang et al. 2001) and supercomplexes including PSI, *cyt b₆f* and FNR were isolated from *Chlamydomonas* (Iwai et al. 2010). FNR likely provides a binding site for ferredoxin (Fd) localized in the vicinity of the Q_i site of *cyt b₆f* (Joliot et al. 2004). On this basis, a structural model for cyclic electron flow has been proposed in which electrons are trapped within supercomplexes that associate *cyt b₆f*, FNR, PGR5 and PGRL1 (cyclic configuration (Joliot and Johnson 2011)). When FNR is not bound to *cyt b₆f* (linear configuration), electrons would be lost for cyclic electron flow and transferred to the Benson–Calvin cycle via NADPH. The equilibration between linear and cyclic electron flows would rely on the redox poise of the stroma, an accumulation of NADPH putatively inducing the binding of FNR to the *cyt b₆f* complex and thus a shift from the linear to the cyclic mode.

In this work, we have compared the efficiency of the cyclic process in the presence or absence of iodoacetamide that has been characterized as an inhibitor of the “dark” reactions of the photosynthetic process, especially CO₂ fixation (Kohn 1935). In the presence of iodoacetamide, we observed that illumination under weak far-red light induces a faster and larger NPQ than that observed under saturating light in the absence of inhibitor. As expected from our bifurcated model of electron transfer in the stroma, a full inhibition of electron flow toward the Benson–Calvin cycle

leads to a large redirection of the electron flow toward the PGR5-mediated cyclic pathway.

Materials and methods

Experiments were performed on mature spinach leaves (*Spinacia oleracea*) or on Arabidopsis leaves. Arabidopsis WT plants (Columbia GL1) and the *pgr5* mutant were a kind gift from Toshiharu Shikanai (Munekage et al. 2002). Arabidopsis plants were grown with a 14-hour photoperiod at a light intensity of 50 $\mu\text{mol photons m}^{-2} \text{s}^{-1}$. Spinach and Arabidopsis leaves were adapted in the dark for more than 2 h prior to analysis. $\sim 5 \times 10$ mm leaf fragments were infiltrated with an isotonic 0.15 M sorbitol buffer by depressurisation in a 20 ml syringe, and further used for spectroscopic experiments. During experiments, air was continuously flowed into the measuring cuvette to avoid CO_2 or O_2 limitation. As the experiments presented here were performed on infiltrated leaves, the air space localized in the spongy mesophyll cells is filled with buffer, which could perturb CO_2 and O_2 exchange. Nevertheless, under such conditions, the PSII photochemical yield reached typical values around ~ 0.14 after 10 min illumination ($k_{\text{PSII}} = 1,000 \text{ s}^{-1}$). It gives a photochemical turnover of about $\sim 140 \text{ s}^{-1}$, close to the maximum value reported for linear electron flow in intact leaves. From this, we concluded that photosynthetic processes were not significantly affected by the infiltration with isotonic sorbitol buffer.

Inhibitors were purchased from Sigma and added to the infiltration buffer at concentrations indicated below. Iodoacetamide (IA) was used as an inhibitor of the Benson–Calvin cycle. Iodoacetyl radical reacts irreversibly with free –SH groups of Cys residues in proteins and therefore inhibits several enzymes involved in the Benson–Calvin cycle: phosphoribulokinase, fructose 1,6-bisphosphatase, sedoheptulose 1,7-bisphosphatase and GAPDH (see Ferri et al. (1981) for the latter). In our hands, we confirmed the slowness of penetration of this poison in intact cells of unicellular algae as reported in (Kohn 1935), and we would similarly recommend the use of high concentrations (up to 10 mM) and long incubation times (1–2 h). In spinach leaves, however, we found 10 min incubation after infiltration of the leaves with 4 mM of iodoacetamide in 0.15 M sorbitol led to a complete inhibition of the Benson–Calvin cycle, and we estimated that 2 mM addition led to 90 % inhibition.

Spectroscopic measurements (fluorescence yield and absorbance changes were measured using a JTS-10 spectrophotometer (Bio-Logic). The fluorescence yield was probed using weak detecting flashes (420 nm) of 4 μs

duration with negligible actinic effects. Green and far red actinic illumination was provided by LEDs peaking at 540 nm ($150 \mu\text{E m}^{-2} \text{s}^{-1}$) and 740 nm ($500 \mu\text{E m}^{-2} \text{s}^{-1}$), respectively. It is worth pointing out that green and far-red light are poorly absorbed, i.e., also homogeneously distributed throughout the leaves, explaining the high intensities used. Pulses of saturating light are provided by LEDs peaking at 620 nm ($6,500 \mu\text{E m}^{-2} \text{s}^{-1}$). Blue detecting flashes and green and far-red actinic illumination were provided on the upper face of the leaf. Being strongly absorbed, blue detecting flashes probe the fluorescence yield in a layer of limited thickness (palisade cells) localized on the upper face of the leaf. This layer is excited homogeneously inasmuch as the green actinic light is weakly absorbed. PSII photochemical rate constant was estimated by measuring the kinetics of fluorescence rise in the presence of DCMU. PSI photochemical rate constant ($k_{\text{PSI}} = 100 \text{ s}^{-1}$ in green light, $k_{\text{PSI}} = 40 \text{ s}^{-1}$ in far-red light) is estimated on the basis of the rise time of the membrane potential measurement (520 nm absorption change) in the presence of DCMU according to the method described in (Joliot and Joliot 2002). By comparing the data obtained with and without DCMU, we have estimated that green light excites PSI and PSII about equally ($k_{\text{PSI}} = k_{\text{PSII}} = 100 \text{ s}^{-1}$).

NPQ was computed according to the formula: $(F_m - F_m')/F_m'$ where F_m is the maximum fluorescence level on a dark adapted sample and F_m' the maximum fluorescence level measured during the course of the illumination. F_m and F_m' were measured at the end of a saturating pulse (200 ms duration) provided by several LEDs (peak emission at 620 nm, $6,000 \mu\text{mol photons m}^{-2} \text{s}^{-1}$). Photosystem II photochemical yield is measured using the formula $(F_m' - F')/F_m'$, where F' is the fluorescence yield measured 50 μs before the pulse of saturating light (see above). The maximum PSII yield $(F_m - F_0)/F_m$, measured on leaves adapted in the dark for more than 2 h varies between 0.78 and 0.83.

P_{700} redox state is determined by measuring the absorption changes at 705 nm using short detecting flashes of 12 μs duration (Joliot and Johnson 2011).

Our spectroscopic instruments are highly sensitive and the error bars are generally smaller than the symbols used in the Figures. In our hands, the highest reproducibility between experiments is obtained when repeating experiments on different fragments from the same leaf. When experiments are compared with and without iodoacetamide or with or without nigericin, they were performed on neighboring fragments of the same leaf that are in the same physiological state. When comparing various leaves, some small physiological differences are generally observed. However, the effect of inhibitor addition was similar in each different sample.

Results and discussion

We have investigated the effect of 4 mM iodoacetamide (IA) on the photosynthetic activity of spinach leaves. In each experiments, depicted in Fig. 1, spinach leaves were dark adapted for 2 h prior to a continuous illumination of 3 min (curves 1 and 3). Figure 1 also shows the curves obtained during a second illumination delivered to the same sample after a 5 min dark relaxation after the first illumination (curves 2 and 4). The yield of photosystem II (left panels) and non-photochemical quenching (NPQ, right panels) have been plotted against the time of illumination after the onset of a green (top panels) or far-red (bottom panels) illumination. While far-red light specifically excites PSI, green light is equally distributed between PSI and PSII. Each 5 s during the course of the illumination, a pulse of saturating light of 100 ms duration was used to probe the maximum fluorescence yield.

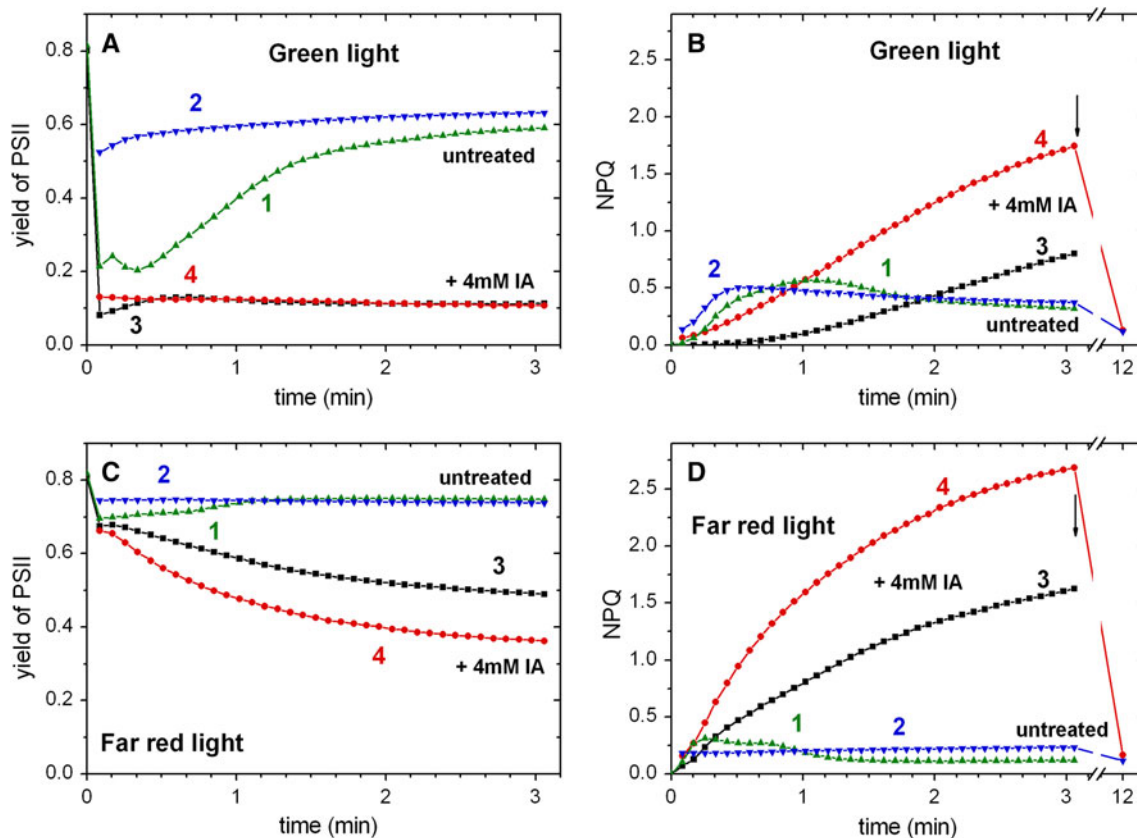


Fig. 1 Yield of photosystem II (left panels) and NPQ (right panels) measured during the course of a green (top panels) or a far-red (bottom panels) illumination in the control (curves 1 and 2) or in the presence of iodoacetamide (curves 3 and 4). Downward arrows show the time the light was turned off. Both experiments were performed on neighboring fragments of the same leaf. In top panels a and b, curves 1 the yield of PSII (a) and NPQ (b) are measured on leaf fragments, pre-adapted in the dark for more than 2 h, and then illuminated with green light ($k_{\text{PSI}} \sim k_{\text{PSII}} \sim 100 \text{ s}^{-1}$) and saturating

Under PSII + PSI illumination, iodoacetamide blocks linear electron flow

Experiments in Fig. 1a show the induction phase of photosynthesis. Under a green illumination of medium intensity (about 100 photons absorbed per PSI and PSII per second, $k_{\text{PSII}} \sim k_{\text{PSI}} \sim 100 \text{ s}^{-1}$), and in the absence of inhibitor (curve 1), the PSII yield first decreases abruptly after 5 s of illumination, then increases steadily during the first minutes of illumination, reflecting the activation of the Benson–Calvin cycle. Despite the infiltration of leaves, the activation of the Benson–Calvin cycle is quite similar to that observed on non-infiltrated leaves. The large yield observed at the onset of the second illumination (curve 2) shows that the Benson–Calvin cycle has not been significantly deactivated during the 5 min dark period that separated the two illuminations. Addition of 4 mM IA (15 min incubation time) blocks the induction phase of photosynthesis, inducing a

pulses of 200 ms duration, 5 s apart, to probe F_m . Curve 2 the same leaf fragment is submitted to a second illumination after 5 min of dark adaptation. Panels c and d, yield of PS II (c) and NPQ (d) measured on a fragment of the same leaf as in panels a and b. Curve 1 same protocol as in panels a and b but the leaf fragment is illuminated under far-red light ($k_{\text{PSII}} \sim 4 \text{ s}^{-1}$ and $k_{\text{PSI}} \sim 40 \text{ s}^{-1}$). Curves 3 and 4 show the results obtained on 4 mM iodoacetamide infiltrated leaves during a first illumination (curve 3) or a second illumination (curve 4) 5 min after a dark relaxation

large and constant inhibition of the PSII yield (curve 3 and 4), as expected from an alkylating agent reacting irreversibly with cysteine residues, therefore hindering the thioredoxin activation of the Benson–Calvin enzymes. No further inhibition of the yield is observed for longer periods of incubation (up to 1 h) or in the presence of 10 mM IA (not shown), suggesting that under such conditions, the Benson–Calvin cycle is fully inhibited. The ratio of the yield measured in the presence of inhibitor and the maximum yield (Q_A fully oxidized) is $0.12/0.82 = 0.15$, giving a remaining flow of $0.15 \times 100 \text{ s}^{-1} = 15 \text{ s}^{-1}$. The activity of malate dehydrogenase (malate shunt) being as well very likely inhibited by iodoacetamide, we ascribe this residual rate to the direct oxidation of primary PSI acceptors by oxygen (Mehler reaction), as shown in (Radmer and Kok 1976). Figure 1b shows the kinetics of NPQ formation obtained in the same experiment as in Fig. 1a. In the absence of inhibitor, a first NPQ increase (curve 1) that peaks after about 1 min of illumination is followed by a decrease that correlates with the activation of the Benson–Calvin cycle. A faster increase in NPQ is observed during the second illumination (curve 2), likely due to the presence of zeaxanthin formed during the first illumination and still present after 5 min of darkness. Addition of 4 mM IA induces a large inhibition of the initial rise in NPQ (curve 3). During the course of illumination, however, NPQ slowly increases. In the dark, most of the NPQ relaxes in 12 min (see straight red line through the break in the time scale) suggesting that the mechanism involved in the quenching is mainly of the qE type, quickly reversible in the dark.

Under PSI illumination, iodoacetamide stimulates NPQ

In Fig. 1c, d the leaves were illuminated under far-red light, specific to PSI ($k_{\text{PSI}} \sim 40 \text{ s}^{-1}$; $k_{\text{PSII}} \sim 4 \text{ s}^{-1}$), to which was superimposed a series of light pulses 5 s apart to probe F_m . In the absence of inhibitor (curve 1 and 2 in Fig. 1c), after 2 min of illumination, the PSII yield reaches a steady state value of 0.75, a value slightly lower (91 %) than the initial level measured on the dark adapted leaf, showing that most PSII centers stay in their ‘open’ state under far-red light. In the presence of inhibitor (curve 3 and 4), the PSII yield slowly decreases down to a value of 0.36 (~ 50 % of the initial level) at the end of the second illumination period (curve 4). In the absence of inhibitor, the kinetics of NPQ formation (Fig. 1d curves 1 and 2) shows a peak of smaller amplitude than that observed under green light (Figure 1b curves 1 and 2). A very low NPQ level (0.24) is reached at steady states at the end of the second illumination, only half of which relaxes in 12 min. It shows that a negligible amount of qE quenchers is generated under far-red light in the absence of inhibitors. Addition of IA largely enhances NPQ formation, reaching a value of

2.7 at the end of the second illumination (curves 3 and 4). Most of this NPQ relaxes in ~ 12 min decaying to a level similar to that observed in the absence of inhibitor (see red line), again suggesting that the mechanism involved in the quenching is mainly of qE type, quickly reversible in the dark.

In order to check if NPQ measured under far-red light in the presence of IA is actually dependant on the formation of the pH gradient (qE quenching), we have analyzed the kinetics of NPQ formation and PSII yield in the presence of IA and of increasing concentrations of nigericin (Fig. 2). Nigericin is a proton/potassium ion exchanger that specifically collapses the proton gradient and decreases NPQ (Gilmore and Björkman 1995). In Fig. 2b, a significant inhibition of NPQ is observed for 0.2 μM nigericin while an almost complete inhibition is reached for a concentration of 1 μM . As expected, NPQ relaxation in the dark is accelerated by nigericin (see the yield measured 10 s and 50 s after switching off the light). We thus conclude that the large NPQ generated under far-red light is predominantly of qE type and reflects a rapid acidification of the lumen generated by an efficient cyclic process. In Fig. 2a (same experiment as in Fig. 2b), the yield of PSII has been measured in the presence of nigericin. PSII yield increased when increasing the concentration of nigericin. During the course of the far-red illumination with IA, because the residual rate constant (attributed to the Mehler reaction, see above, representing an electron outflow of $\sim 15 \text{ s}^{-1}$) is faster than the PSII photochemical rate constant (electron inflow $\sim 4 \text{ s}^{-1}$), one expects that most of intersystem electron carriers, including Q_A , stay in their oxidized form.

A stimulation of NPQ in low light has been reported in an Arabidopsis mutant devoid of ATPase (Dal Bosco et al. 2004). We have thus checked if the luminal acidification, detected as an increase in NPQ, was associated to an inhibition of the ATPase by IA. Following a saturating light pulse, the decay kinetics of the membrane potential (monitored as an electrochromic shift of carotenoids at 520 nm) displayed a fast phase completed in ~ 100 ms, reflecting proton translocation associated with ATP synthesis (Junge et al. 1970; Joliot and Joliot 2008). The kinetics and amplitude of the fast decay in absorbance at 520 nm being similar in both treated and untreated samples (see Supplementary Information and comments therein), we thus conclude that the large pH-dependant NPQ observed in the presence of IA is not related to an inhibition of ATPase but is rather related to an enhancement of cyclic electron flow.

In Fig. 3, the effects of the two light sources, saturating pulses and far-red light were discriminated by switching off the far-red light. It is worth noting that different amplitudes of NPQ formation are observed when comparing independent experiments (after 3 min of illumination: NPQ = 2.5 in curve 1 Fig. 3 and NPQ = 1.5 in curve

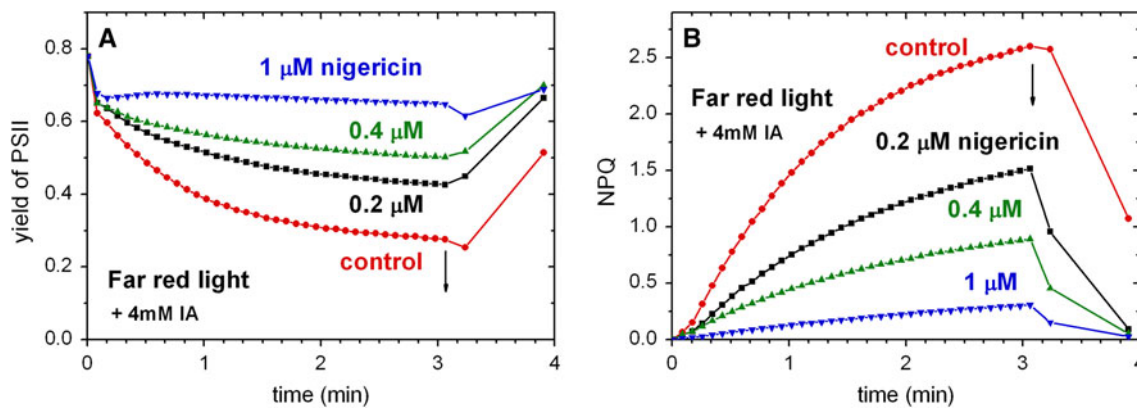


Fig. 2 Effect of nigericin on the yield of PSII (*left*) and NPQ (*right*). The experiment was performed in the same conditions as in Fig. 1c, d. Downward arrows show the NPQ relaxation 10 and 50 s after the light was turned off. PSII yield (a) and NPQ (b) have been measured

3 Fig. 1d). It shows some variability among spinach leaves. However, reproducible amplitudes are obtained when comparing fragments from the same leaf. Doubling the far-red light intensity does not increase NPQ (not shown), showing that, under such conditions of illumination, the rate of NPQ formation was limited by a dark reaction. Curve 2 shows the kinetics of NPQ induced by the sole pulse series, 5 s apart, in the absence of far-red illumination. These repetitive pulses alone induce a slow and very small linear increase in NPQ. Interestingly, at the end of the pulse series, NPQ does not relax in the dark but keeps on increasing to reach the same level as in curve 1 after 12 min of darkness (black line). Thus, illumination with saturating pulses induces a weak quenching, slowly reversible, whether far-red light was present or not. This quenching is likely of the type photoinhibition (qI type) rather than state transition (qT) inasmuch as a far-red illumination would favor state I (unquenched state) rather than state II (quenched state).

NPQ formation under far-red light in the presence of iodoacetamide depends upon the presence of PGR5

As discussed above, the large NPQ observed under far-red illumination in the presence of IA reflects the formation of a large proton gradient induced by an efficient cyclic electron flow rather than an inhibition of ATPase. In Fig. 4, we have compared the kinetics of NPQ formation and PSII yield on leaves from *Arabidopsis* wild type and from the *pgr5* mutant (Munekage et al. 2002). In the *pgr5* mutant illuminated under far-red light in the presence of IA, the initial rate of NPQ formation is considerably decreased (about tenfold) and the PSII yield is less affected than in the WT. The slow PSII electron flow ($<4 \text{ s}^{-1}$) operating under far-red light is likely coupled to the Mehler reaction,

in the presence of 4 mM iodoacetamide during the course of a far-red illumination, and 10 and 50 s after the end of illumination. The 4 experiments have been performed on fragments of the same leaf dark adapted for more than 2 h

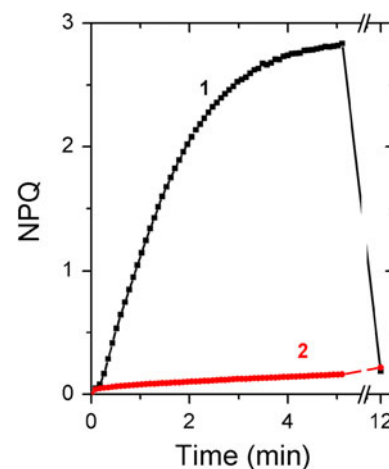


Fig. 3 Effect of saturating pulses on NPQ formation in the presence of iodoacetamide under different conditions of illumination. Curves 1, 2 are obtained on fragments of the same leaf. Curve 1 NPQ formation upon illumination with far-red light with saturating pulses 5 s apart (same conditions as in Fig. 1d). Curve 2 NPQ formation upon illumination by a series of pulses 5 s apart (no far-red light in this case). NPQ relaxation in the dark has been measured after 12 min (see black and red lines)

as the Benson–Calvin cycle is inhibited by IA. Such a water–water cycle (or pseudocyclic photophosphorylation) is likely to generate a weak proton gradient accounting for the small increase in NPQ observed in the *pgr5* mutant. On this basis, we confirm that there is no significant cyclic electron flow in the *pgr5* mutant.

Iodoacetamide enhances cyclic electron flow under PSI illumination

In Fig. 5 we have quantified the efficiency of the cyclic process in the presence or absence of iodoacetamide by measuring the kinetics of P_{700} oxidation, according to a

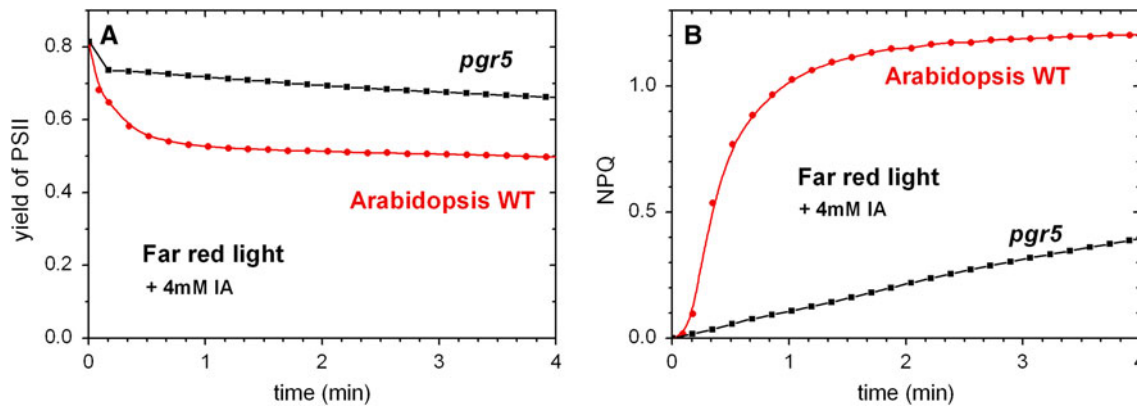


Fig. 4 Effect of the presence or absence of PGR5 in Arabidopsis leaves on the yield of PSII (left) and NPQ (right) in the same conditions as in Figs. 1c, d and 2, downward arrows show the time

when the light was turned off. PSII yield (a) and NPQ (b) have been measured in the presence of 4 mM iodoacetamide during the course of a far-red illumination

method described previously in (Joliot and Joliot 2002; Joliot and Johnson 2011). Curves 1 and 2 obtained for untreated spinach leaves are similar to those we previously obtained in Arabidopsis (Joliot and Joliot 2002; Joliot and Johnson 2011). The two different preillumination protocols used for curves 1 and 2 aim at preconditioning the leaves in the linear or cyclic electron flows respectively (Joliot and Johnson 2011). In curve 1, a spinach leaf infiltrated without IA has been illuminated for more than 5 min under far-red light ($k_{\text{PSI}} \sim 40 \text{ s}^{-1}$). After far-red preillumination, the leaf was subjected to a pulse of saturating light (200 ms duration) that fully reduced the PQ pool. Following a 2 s dark adaptation, P_{700} oxidation is monitored upon far-red illumination ($k_{\text{PSI}} \sim 40 \text{ s}^{-1}$). The kinetics shows a lag phase that has been ascribed to the oxidation of the PQ pool. Assuming that during the lag (0.3 s), PSI operates close to its maximum efficiency, the number of electrons transferred via PSI is about $\sim 0.3 \times 40 = 12$ electrons, a number roughly corresponding to the pool size of PSI secondary electron donors (PQ pool) previously reduced by the 200 ms pulse of saturating light. We thus confirm that, following a long far-red preillumination, the photosynthetic apparatus operates according to the linear mode (Joliot and Johnson 2011). Curve 2 has been obtained in the same conditions as curve 1 except that the saturating illumination lasted for 15 s instead of 200 ms. Kinetics of P_{700} oxidation, including the lag phase, is about ~ 2.5 times longer after the long pulse than after the short pulse. According to (Joliot and Johnson 2011), this slowing down does not reflect a PSI acceptor side limitation but rather implies that a fraction of the electrons transferred to PSI acceptors are transferred back to the PQ pool via the cyclic process. The ~ 2.5 -fold increase in the lag duration implies that during the first second of illumination $\sim 2.5 \times 12 = 30$ electrons are transferred through the PSI centers. Thus, during the lag, ~ 18 and ~ 12 electrons are transferred via the cyclic

and linear processes, respectively. Under such conditions, $\sim 2/3$ of the electrons transferred at the acceptor side of PSI are therefore engaged in the cyclic process and $\sim 1/3$ in the linear process. Curve 3 shows the kinetics of P_{700} oxidation measured in the presence of 4 mM IA (same protocol as in curve 1). Following the 200 ms pulse, the kinetics shows a much longer lag period than in the absence of inhibitor ($>10 \text{ s}$ duration). Applying a 20 ms saturating pulse at the end of the far-red illumination induces a full oxidation of P_{700} (green arrow). It rules out a possible limitation of electron transfer at the acceptor side of PSI. In the presence of inhibitor, the duration of the lag is ~ 30 times longer than in curve 1 (linear mode). On this basis, we estimate that the probability for reduced PSI electron acceptors to be oxidized via the cyclic pathway is 20–30 times larger than via the linear pathway. This implies that most of PSI centers contribute to the cyclic process. The unprecedented efficiency of the cyclic process in the presence of iodoacetamide explains the fast rate of NPQ formation reported in Fig. 1d, curves 3 and 4.

In the presence of iodoacetamide, a green illumination that excites both PSI and PSII reduces F_A and F_B in PSI

In Fig. 5, curve 4 shows the kinetics of P_{700} measured in the presence of 4 mM IA using the same preillumination protocol than that is used in curve 3 except that at time zero the leaf is illuminated with green light ($k_{\text{PSII}} \sim k_{\text{PSI}} \sim 100 \text{ s}^{-1}$) and not far-red light. Following a small peak of oxidation, and similarly to that observed in far-red light (curve 3), P_{700} stays mainly reduced throughout the period of the green illumination. However, contrary to that observed on curve 3, a 20 ms pulse of saturating light superimposed to the green illumination does not induce a significant P_{700} oxidation, showing a limitation of electron transfer at the acceptor side of PSI. It implies that most of

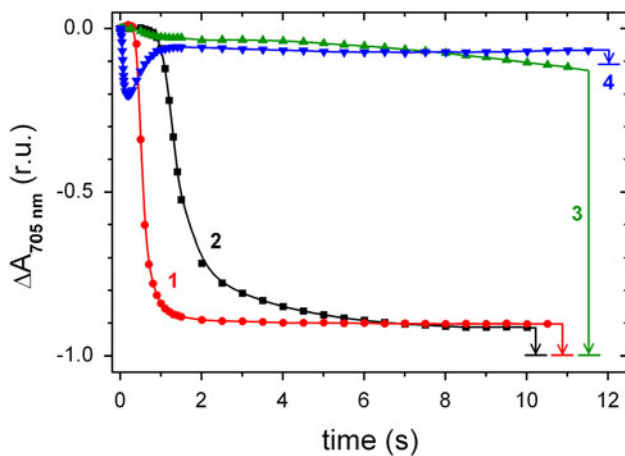


Fig. 5 Evaluation of cyclic electron flow using P_{700} kinetics (absorbance changes at 705 nm). Preillumination protocols aim at preconditioning the system in linear or cyclic modes. *Curve 1* a dark adapted leaf fragment is preilluminated for 5 min under far-red light ($k_{PSI} \sim 40 \text{ s}^{-1}$), this preillumination ends with a pulse of saturating light (200 ms duration). After a dark adaptation of 2 s, P_{700} oxidation is measured upon illumination with the same far-red light. At the end of the far-red illumination the maximum P_{700}^+ level is measured by delivering a pulse of saturating light (20 ms duration), see downward arrows. The amplitude of the P_{700}^+ signal is normalized to the total PSI concentration. *Curve 2*: same as curve 1 but the leaf is illuminated for 15 s (instead of 200 ms) under saturating red light at the end of the 5 min far-red illumination. *Curve 3* same as curve 1 but in the presence of 4 mM iodoacetamide. *Curve 4* same as curve 3 but P_{700} oxidation is measured under green light ($k_{PSII} \sim k_{PSI} \sim 100 \text{ s}^{-1}$) instead of far-red light

the PSI acceptors were reduced by the continuous green light prior to the pulse. We propose that under green illumination, the large electron flow originating from PSII induces the reduction of most of the PSI electron acceptors, leading to back reactions and a block of PSI photochemistry and cyclic electron flow. Such an obstruction of linear and cyclic electron flows under green illumination also accounts for the low PSII yield (Fig. 1a, curve 3) and the slow initial rate of NPQ formation (Fig. 1b, curve 3). Back reactions between P^+ and F_A^- and F_B^- are multiphasic with rate constants in the range of $5\text{--}20 \text{ s}^{-1}$ (Brettel 1997). Such back reactions do not compete with the forward reduction of P_{700}^+ by electrons produced at the level of PSII under green illumination ($k_{PSII} \sim 100 \text{ s}^{-1}$). We thus conclude that, in the presence of IA, F_A and F_B are reduced in green light. Under such conditions, back reactions are expected to occur between P^+ and A_1^- or F_X^- , depending upon the equilibrium constant between these two electron carriers. Under far-red illumination, the PSII photochemical rate constant ($k_{PSII} \sim 4 \text{ s}^{-1}$) is slower than the rate constant of the electron leak via the Mehler reaction ($\sim 15 \text{ s}^{-1}$). Under such conditions, even in the presence of IA, the weak electron flow generated by PSII is unlikely able to steadily reduce F_A , F_B , thus preventing the occurrence of back

reactions. On the other hand, the efficient cyclic electron flow observed in these conditions requires that most of $NADP^+$ is reduced to NADPH (Joliot and Johnson 2011). This is compatible with the large equilibrium constant (>1000) between F_A/F_A^- ($E_m = -530 \text{ mV}$) and $NADP^+/NADPH$ ($E_m = -320 \text{ mV}$). We can therefore reasonably estimate that the redox poise of the stroma in the presence of IA and far-red light is in between these two midpoint potentials, say around -420 mV . Such a moderate reducing pressure from far-red light would leave $\sim 98 \%$ of F_A oxidized but would maintain NADPH 98 % reduced, therefore, optimizing the rate of the cyclic process.

Concluding remarks

Inhibition of the Benson–Calvin cycle by iodoacetamide provides an efficient tool to stimulate, with far-red light, cyclic electron flow around PSI. It confirms that this process is controlled by PGR5 and the redox state of stromal reductants (Arnon and Chain 1975; Hosler and Yocum 1987; Allen 2003; Breyton et al. 2006; Alric 2010; Alric et al. 2010; Joliot and Johnson 2011; Kramer and Evans 2011). Under such conditions, a large acidification of the lumen is evidenced as a large nigericin-sensitive NPQ (qE component). As emphasized in (Alric 2010), the optimal conditions to observe the maximal cyclic electron flow rate are not easily assessed experimentally. The large efficiency of the cyclic process we observed with far-red illumination in the presence of IA is the result of a subtle balance between the rate of PSII electron flow, sufficient to maintain the reducing pressure on the electron transport chain (and ultimately on NADPH), and the rate of electron leaks, probably via the Mehler reaction, sufficient to prevent the reduction of F_A and thus the occurrence of back reactions.

Acknowledgments The authors are indebted to Fabrice Rappaport for a critical reading of the manuscript.

References

- Allen JF (1992) Protein phosphorylation in regulation of photosynthesis. *Biochim Biophys Acta* 1098(3):275–335
- Allen JF (2003) Cyclic, pseudocyclic and noncyclic photophosphorylation: new links in the chain. *Trends Plant Sci* 8(1):15–19
- Alric J (2010) Cyclic electron flow around photosystem I in unicellular green algae. *Photosynth Res* 106(1–2):47–56
- Alric J, Lavergne J et al (2010) Redox and ATP control of photosynthetic cyclic electron flow in *Chlamydomonas reinhardtii* (I) aerobic conditions. *Biochim Biophys Acta* 1797(1):44–51
- Arnon DI, Chain RK (1975) Regulation of ferredoxin-catalyzed photosynthetic phosphorylations. *Proc Natl Acad Sci USA* 72(12):4961–4965
- Arnon DI, Allen MB et al (1954) Photosynthesis by isolated chloroplasts. *Nature* 174(4426):394–396

- Brettel K (1997) Electron transfer and arrangement of the redox cofactors in photosystem I. *Biochimica et Biophysica Acta (BBA)—Bioenergetics* 1318(3):322–373
- Breyton C, Nandha B et al (2006) Redox modulation of cyclic electron flow around photosystem I in C3 plants. *Biochemistry* 45(45):13465–13475
- Clark RD, Hawkesford MJ et al (1984) Association of ferredoxin-NADP + oxidoreductase with the chloroplast cytochrome b-f complex. *FEBS Lett* 174(1):137–142
- Dal Bosco C, Lezhneva L et al (2004) Inactivation of the chloroplast ATP synthase gamma subunit results in high non-photochemical fluorescence quenching and altered nuclear gene expression in *Arabidopsis thaliana*. *J Biol Chem* 279(2):1060–1069
- Ferri G, Iadarola P et al (1981) Chloroplast glyceraldehyde-3-phosphate dehydrogenase (NADP +). Reactivity of essential cysteine residues in holo- and apoenzyme. *Biochim Biophys Acta* 660(2):325–332
- Finazzi G, Rappaport F (1998) In vivo characterization of the electrochemical proton gradient generated in darkness in green algae and its kinetic effects on cytochrome b6f turnover. *Biochemistry* 37(28):9999–10005
- Gilmore AM, Björkman O (1995) Temperature-sensitive coupling and uncoupling of ATPase-mediated, nonradiative energy dissipation: similarities between chloroplasts and leaves. *Planta* 197(4):646–654
- Hald S, Nandha B et al (2008) Feedback regulation of photosynthetic electron transport by NADP(H) redox poise. *Biochim Biophys Acta* 1777(5):433–440
- Harbinson J, Foyer CH (1991) Relationships between the efficiencies of photosystems I and II and stromal redox state in CO₂-free air. *Plant Physiol* 97(1):41–49
- Harbinson J, Woodward FI (1987) The use of light-induced absorbance changes at 820 nm to monitor the oxidation state of P-700 in leaves. *Plant Cell Environ* 10(2):131–140
- Heber U (1969) Conformational changes of chloroplasts induced by illumination of leaves in vivo. *Biochimica et Biophysica Acta (BBA)—Bioenergetics* 180(2):302–319
- Horton P, Ruban AV et al (1996) Regulation of Light Harvesting in Green Plants. *Annu Rev Plant Physiol Plant Mol Biol* 47:655–684
- Hosler JP, Yocum CF (1987) Regulation of Cyclic Photophosphorylation during Ferredoxin-Mediated Electron Transport : effect of DCMU and the NADPH/NADP Ratio. *Plant Physiol* 83(4):965–969
- Iwai M, Takizawa K et al (2010) Isolation of the elusive supercomplex that drives cyclic electron flow in photosynthesis. *Nature* 464(7292):1210–1213
- Joliot P, Johnson GN (2011) Regulation of cyclic and linear electron flow in higher plants. *Proc Natl Acad Sci USA* 108(32):13317–13322
- Joliot P, Joliot A (2002) Cyclic electron transfer in plant leaf. *Proc Natl Acad Sci USA* 99(15):10209–10214
- Joliot P, Joliot A (2008) Quantification of the electrochemical proton gradient and activation of ATP synthase in leaves. *Biochim Biophys Acta* 1777(7–8):676–683
- Joliot P, Beal D et al (2004) Cyclic electron flow under saturating excitation of dark-adapted *Arabidopsis* leaves. *Biochim Biophys Acta* 1656(2–3):166–176
- Junge W, Rumberg B et al (1970) The necessity of an electric potential difference and its use for photophosphorylation in short flash groups. *Eur J Biochem* 14(3):575–581
- Kohn HI (1935) Inhibition of photosynthesis in *Chlorella pyrenoidosa* by the iodo-acetyl radical. *J Gen Physiol* 19(1):23–34
- Kok B, Joliot P et al (1969) Electron transfer between the photoacts. In: Metzner H (ed) *Progress in photosynthesis research*, vol 2., pp 1042–1056
- Kramer DM, Evans JR (2011) The importance of energy balance in improving photosynthetic productivity. *Plant Physiol* 155(1):70–78
- Li XP, Gilmore AM et al (2004) Regulation of photosynthetic light harvesting involves intrathylakoid lumen pH sensing by the PsbS protein. *J Biol Chem* 279(22):22866–22874
- Munekage Y, Hojo M et al (2002) PGR5 is involved in cyclic electron flow around photosystem I and is essential for photoprotection in *Arabidopsis*. *Cell* 110(3):361–371
- Ott T, Clarke J et al (1999) Regulation of the photosynthetic electron transport chain. *Planta* 209(2):250–258
- Radmer RJ, Kok B (1976) Photoreduction of O(2) Primes and Replaces CO(2) Assimilation. *Plant Physiol* 58(3):336–340
- Ruban AV, Pascal AA et al (2002) Activation of zeaxanthin is an obligatory event in the regulation of photosynthetic light harvesting. *J Biol Chem* 277(10):7785–7789
- Rutherford AW, Osyczka A et al (2012) Back-reactions, short-circuits, leaks and other energy wasteful reactions in biological electron transfer: redox tuning to survive life in O(2). *FEBS Lett* 586(5):603–616
- Sazanov LA, Burrows P et al (1996) Detection and characterization of a complex I-like NADH-specific dehydrogenase from pea thylakoids. *Biochem Soc Trans* 24(3):739–743
- Seelert H, Poetsch A et al (2000) Structural biology. Proton-powered turbine of a plant motor. *Nature* 405(6785):418–419
- Siefermann D, Yamamoto HY (1975) Properties of NADPH and oxygen-dependent zeaxanthin epoxidation in isolated chloroplasts: a transmembrane model for the violaxanthin cycle. *Arch Biochem Biophys* 171(1):70–77
- Zhang H, Whitelegge JP et al (2001) Ferredoxin:NADP⁺ oxidoreductase is a subunit of the chloroplast cytochrome b6f complex. *J Biol Chem* 276(41):38159–38165